# INTRODUCING A SCRIPT FOR CALCULATING THE SKY VIEW FACTOR USED FOR URBAN CLIMATE INVESTIGATIONS

## M HÄMMERLE[1], T GÁL[2], J UNGER[2] and A MATZARAKIS[1]

[1]Meteorological Institute, Albert-Ludwigs-University of Freiburg, 79085 Freiburg, Germany
E-mail: martin.haemmerle@meteo.uni-freiburg.de
[2]Department of Climatology and Landscape Ecology, University of Szeged, P.O.Box 653, 6701 Szeged, Hungary

**Summary**: The sky view factor (SVF) is a parameter widely used in several research fields, applied research and planning. It is of crucial importance concerning the energy budget of a certain location. Many methods for calculating the SVF have been developed. In the present study, a selection of methods and models is analyzed in order to find out about possible improvements. Also, a new method using GIS software is introduced. In the city of Szeged fisheye pictures were taken along transects and evaluated. For the images' coordinates, SVF was calculated by numerical models which use a 3D-building database as input. Also, a set of artificial fisheye pictures was created and used for validating the applied methods. The calculations were performed with the models SkyHelios (Matuschek and Matzarakis 2010, Matzarakis and Matuschek 2010), SOLWEIG (Lindberg et al. 2008) and the ArcView SVF-Extension (Gál et al. 2009). The evaluation of the fisheye pictures was done according to the manual Steyn-method (Steyn 1980), RayMan (Matzarakis et al. 2007 2010) and with BMSkyView (Rzepa and Gromek 2006). Additionally, a new ArcView-script has been developed in order to enhance the only manual method (Steyn 1980). The comparison of the obtained results showed a systematic deviation of the SVF values. After including a cosine weighting factor in the differing models, all SVF values corresponded to each other.

**Key words**: urban climate, SVF-calculation methods, comparison

## 1. INTRODUCTION

The sky view factor (SVF or $\psi_s$) is a dimensionless parameter with values between zero and one. It represents the fraction of visible sky on a hemisphere which lays centred over the analyzed location (Oke 1981).

Different sky view factors mean different radiation budgets and accordingly different energy budgets: On a point with a SVF of 1 (the complete sky is visible) under clear sky conditions neither reflected short-wave radiation, nor additional long-wave radiation is received. The radiation budget for an "ideal" site can thus be written as in Fig. 1 (left side) and accordingly the energy budget corresponds to Fig. 1 (right side).

In Fig. 1, $Q^*$ stands for the net radiation budget, $S\downarrow$ is the incoming short-wave radiation (direct solar and diffuse), $S\uparrow$ the outgoing short-wave radiation (reflection), $L\downarrow$ the incoming long-wave radiation (atmospheric downward-radiation), $L\uparrow$ the outgoing long-wave radiation (emission of the surface); $Q_G$ stands for the soil heat flux (energy stored in volumes, e.g. soil, buildings), $Q_H$ is the sensible heat flux (air temperature) and $Q_E$ the latent heat flux (evaporated water).

$$Q^* = S\!\downarrow + S\!\uparrow + L\!\downarrow + L\!\uparrow \qquad\qquad Q^* + Q_G + Q_H + Q_E = 0$$
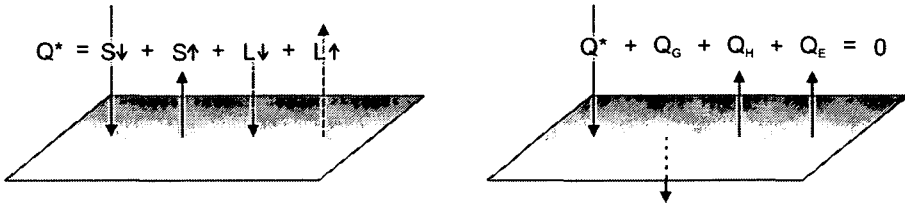
Fig. 1 Schematic summary of the fluxes involved in the radiation budget (left) and energy balance (right) of an "ideal" site (modified after Oke 1987)

If, in contrast, the analyzed location is situated for example in a valley or street canyon (Fig. 2), the radiation budget and the energy budget are changed by
- reflections of short-wave radiation as shown Fig. 2a,
- a decrease in outgoing long-wave radiation as shown Fig. 2b,
- an increase in received long-wave radiation that is emitted by the surfaces which obstruct the sky and consequently
- an altered soil heat flux.

The sky view factor thus plays a crucial role e.g. in urban climatology (Oke 1987), forest climatology (Holmer et al. 2001), human biometeorology (VDI 1998, Matzarakis 2001) etc. It is widely used as an important parameter in modelling thermal phenomena, such as the urban heat island (Unger 2004). Further it can be and it is used in a variety of new fields, e.g. the modeling of ventilation paths, research concerning renewable energy sources (Richert 2010) or urban planning (Lin et al. 2010).

Several numerical models for calculating the sky view factor and several methods for evaluating the SVF have been developed. The aim of this work is to compare and to validate some of these models and methods (see section 3) in order to find out about possible differences in the results and thus to offer a background for improvements.
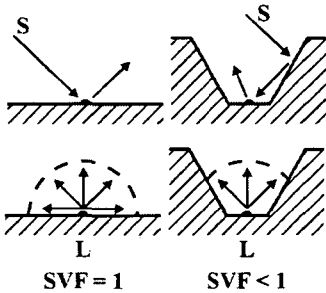
SVF = 1          SVF < 1

Fig. 2 The role of surface geometry in radiation exchange. Comparison of horizontal and convoluted surfaces. S = short-wave radiation, L = long-wave radiation. (modified after Oke 1987)

## 2. STUDY AREA

For calculating the sky view factor with the different models and for validating the calculations, a city on flat terrain would be most convenient. Where there is no noteworthy relief, the computations can be done without including data about the topography and are thus less time-consuming and less prone to errors.

As there was already a 3D-database and a collection of fisheye pictures available (Unger 2006, 2009, Gál et al. 2009), the city of Szeged in South-Hungary (Fig. 3) was chosen for this work.
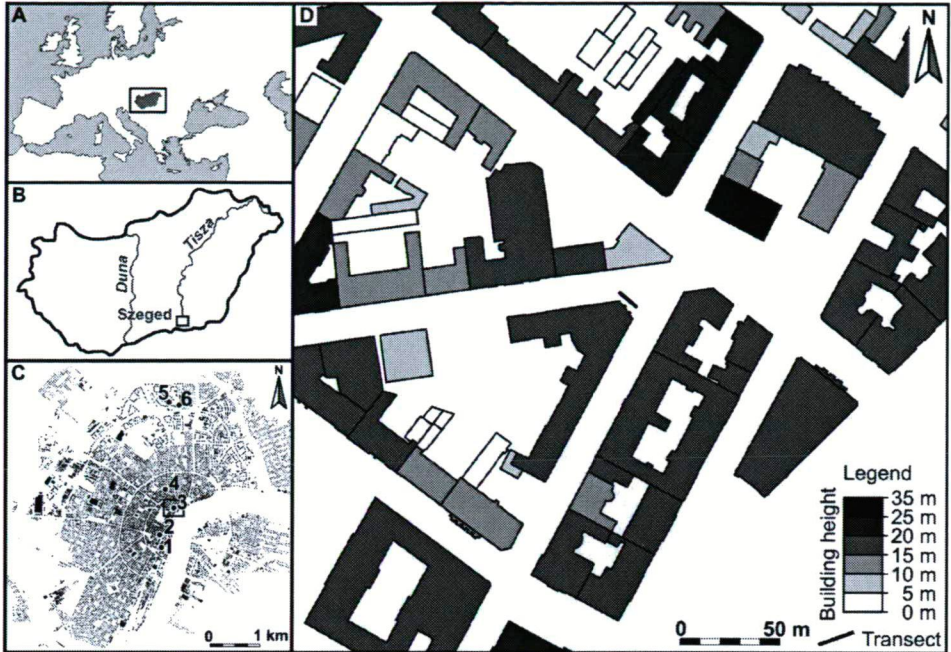
Fig. 3  The location of Hungary in Europe (A), the location of Szeged in Hungary (B), the footprint of Szeged and the locations of transects (C) and the surroundings of transect 3 (D)



Fig. 4  Views of transect 3, from the west (right), from the east (left)

It was intended to cover a variety of different building structures in order to find out how the methods react. As a guideline, the local climate zones (LCZ) as introduced by Stewart (2009) were used. In this paper, only transect 3 is presented (Fig. 3), since all of the important findings can be demonstrated here. The transect lies in the north-eastern intersection of Horváth Mihály street and Deák Ferenc street and consists of the pictures nr. 3023 to 3043 (Fig. 7). It was classified in the LCZ "compact midrise". From the first

observing points, some vegetation in its "leaf on" phase is viewable. The images were taken equidistantly every 0.5 meters.

Fig. 3d shows the surroundings of transect 3 and is intended to be an overview and a help for interpreting and understanding the results. The typical building height in this area is around 15-20 m and the vegetation is represented by only a few trees (Fig. 4).

## 3. METHODS

### 3.1. Fisheye images

The fisheye images were taken with a Nikon Coolpix 4500 digital camera and a Nikon Fisheye Converter FC-E8 0.21x. The camera was mounted on a Gorillapod original tripod. For leveling the camera, a Lenspen panamatic bubble level (Parkside Optical Inc.) was also mounted on the tripod (Fig. 5). This configuration is quite convenient and practical, it can be moved fast and easily and uneven surfaces like gutters are no obstacle for the measurements.

A mask was created to cut the fisheye pictures to 180°. Cutting the images was necessary because the FC-E8 lens have a field of view (FOV) of 189° (Grimmond et al. 2001).

The positions of the images of transect 3 were marked with chalk on the street and then were measured with a Sokkia SET310 theodolite. As reference points, edges of the surrounding buildings were used. The building's coordinates were already available from the 3D building database (Gál et al. 2009).

Fig. 5 Equipment for taking the fisheye pictures

### 3.2. SVF evaluation methods using fisheye photoes

#### 3.2.1. Manual method according to Steyn

This is a very basic method of evaluating fisheye pictures. First, the fisheye picture is printed with an overlain polar grid. In the print, the obstacles are then to be delineated manually. With the help of the polar grid the viewing angle of each annulus is to be counted. After the SVF is calculated for each annulus according to the formulas in Steyn (1980) the values are summed up for the total SVF.

### 3.2.2. "Edit free sky view factor"-tool of RayMan

This RayMan-module (Matzarakis et al. 2007 2010) calculates the SVF after obstacles are digitized in a fisheye picture or loaded directly into the module. After digitizing, the SVF is calculated by counting the sky-pixels and relating them to the total number of pixels in the image.

### 3.2.3. BMSKyView

This software (Rzepa and Gromek 2006, Gál et al. 2007) colours all pixels which are to a certain degree similar to the clicked pixel. A threshold has to be chosen that groups not too many and not too few pixels which are to be coloured. The sky pixels are to be chosen. Some pixels in buildings (e.g. sky-reflecting windows) have to be unmarked after the selection of all sky pixels. The marked pixels are used for the SVF-calculation which is based on the Steyn-method.

### 3.3. New approach: Steyn-method implemented in an ArcView script

To overcome the disadvantages of the manual Steyn-method (material used for the prints, low contrast, tedious and time consuming), an Avenue script was developed in order to evaluate fisheye pictures more easily using GIS-software.

The main difference to the manual Steyn-method is the shift from manual work to digitizing the fisheye images on the computer. For a convenient programming of the ArcView Avenue script, not the obstructed areas are used for the calculation, but the area of visible sky, which is thus to be digitized.

The method uses the same formula as the manual Steyn-method. It first creates a theme of n annular rings (n is user defined, the default is 36) and then calculates the maximum value of SVF for each annular ring ($SVF_{max\,i}$) with

$$SVF_{maxi} = \frac{\pi}{2} \cdot \sin\left(\frac{\pi \cdot (i - 0.5)}{2n}\right) \cdot \cos\left(\frac{\pi \cdot (i - 0.5)}{2n}\right) \tag{1}$$

where n is the count of annular rings, i the number of the actual ring and $\pi$ the mathematical constant Pi.

In the next step, the visible sky is digitized as a new theme. Via intersecting the annular rings with the digitized visible sky theme, $\alpha_i$ (obstructed angle in ring i) is calculated with

$$\alpha_i = \frac{T_{total} - T_{obs}}{\pi \cdot r_2^2 - \pi \cdot r_1^2} \tag{2}$$

where $T_{total}$ is the total area of the annular ring, $T_{obs}$ is the obstructed area in the same ring, $r_1$ and $r_2$ are the radii of the inner and outer limits of the ring, respectively.

Each ring's SVF is then calculated via

$$SVF_i = SVF_{maxi} \cdot \frac{\alpha_i}{2\pi} \tag{3}$$

and finally, all $SVF_i$ are summarized, which results in the total SVF. After this calculation the software writes the SVF value to the screen.

Digitizing the sky is done fast and easily with the script because vegetation can be more easily separated from rooftops on an actively light emitting screen. In addition, zooming in and out of the image is very helpful. The SVF-calculation for the digitized image is done with one click. This method is estimated the fastest for evaluating fisheye images.

As the script is customized for the original pictures of FC-E8 lens with its FOV of 189°, the use is restricted to a certain set of equipment. On the other hand, an extension to meet other general conditions can easily be introduced in the source code of the Avenue script.

### 3.4. SVF compution methods using a 3D building database

#### 3.4.1. SkyHelios

The calculations with SkyHelios (Matuschek and Matzarakis 2010, Matzarakis and Matuschek 2010) were done twice for each transect: First with a raster input file (resolution 0.5x0.5 m), second with a vector input file, both extracted from the 3D building database. SkyHelios works in a similar way to RayMan: A virtual fisheye picture for each observation point is generated based on the 3D input. The image is evaluated following the steps as done by RayMan.

#### 3.4.2. ArcView SVF-Extension

The extension (Unger 2009, Gál et al. 2009) uses a vector-based 3D building data base as input. A point shapefile has been created using the coordinates of the pictures and the SVF-calculation is done for each point in this file. The calculation method is based on Oke's SVF formula for a basin (Oke 1987). The software scans the horizon stepwise by drawing a line and searching for intersections between this line and the buildings. A step size of 1° was chosen and the scanned distance was 200 meters which gives the best results with quite a low calculation time (Unger 2009). The detected obstacles' height is read from the 3D database and the highest building that intersects the scan line is taken for the calculation (Gál et al. 2009).

#### 3.4.3. SOLWEIG

SOLWEIG (Lindberg et al. 2008) calculates the sky view factor on the basis of a shadow casting algorithm as introduced by Ratti and Richens (1999). Due to problems with the software or the computing equipment, the resolution for all transects was 1x1 m.

### 3.5. Method for validation

In addition to the evaluation of real fisheye photos and model runs, some "ideal" fisheye photos were generated. For this purpose, a set of 36 pictures with 36 circles each was created. The pictures simulate an "opening sky": Each consecutive picture has one more additional white ring. This set of pictures stands for a stepwise virtual opening of the sky and leads to a cumulative SVF-calculation from one single visible ring in the centre to full visibility which means a SVF of 1 (Fig. 6).

| Ring 1 visible | Rings 1-18 visible | Rings 1-36 visible |

Fig. 6 Cumulatively „visible" rings as input for validating

The artificial sky rings were evaluated with the three methods RayMan (workflow as above except digitizing the obstacles: the produced artificial fisheye picture was used directly), BMSkyView (workflow as above) and the manual Steyn-method (SVF was calculated in a spread sheet).

## 4. RESULTS

First follows a description of the comparison results for transect 3. Then, the results of the evaluation based on the artificial images are shown and described.

### 4.1. Results for the fisheye images

A line chart was drawn for the transect (Fig. 7). As the points of the transect are equidistantly following a line, a continuous change in SVF can be assumed.
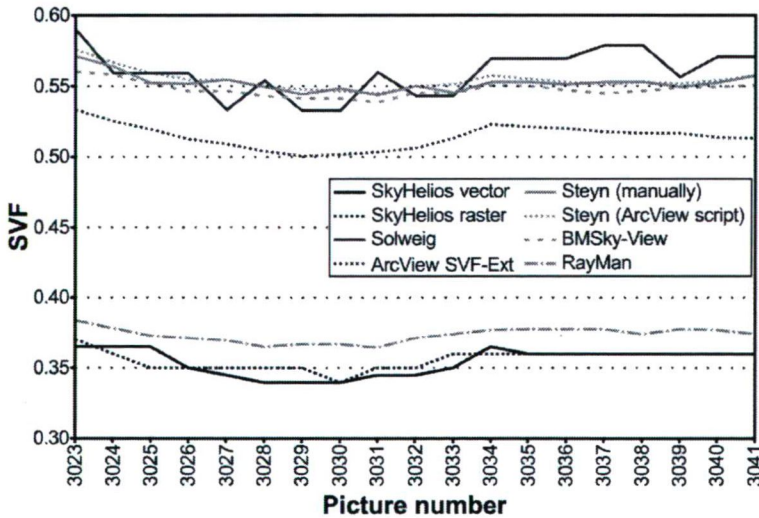


Fig. 7 SVF-diagram for transect 3

Regarding the SVF values, two groups are to be seen: group 1 consists of RayMan and SkyHelios on the one side, group 2 of the SVF-Extension for ArcView, the Steyn-Script for ArcView, Solweig and BMSky-View on the other side.

The range of SVF values is surprisingly small. The minimum value is to find at point 3029 from which the two streets going to the south and west (Fig. 3) are most obstructed by the building along which runs the transect (Fig. 4). On both the starting and ending part of the transect, always one of the intersecting streets is to see which results in higher SVF values.

### 4.2. Results of the validation

The values of the well established Steyn-method are used as reference. They are considered appropriate because the values were calculated in a spreadsheet and are thus "virtual", means: not influenced by any deviations and errors which can occur in fisheye pictures or the evaluation process.
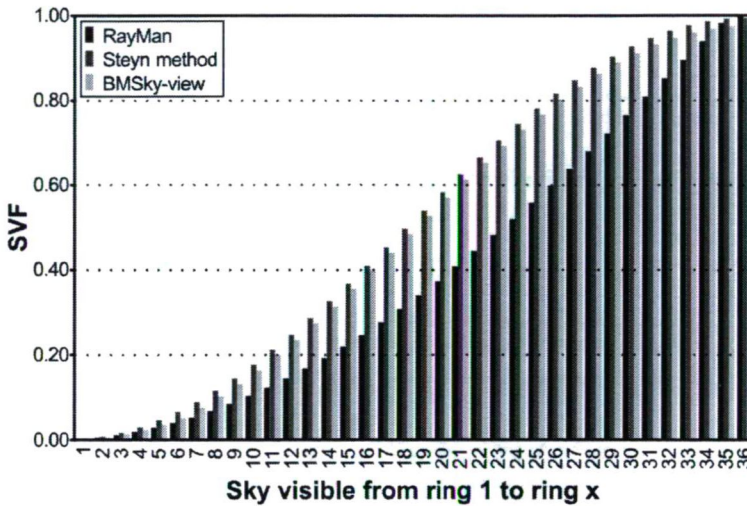


Fig. 8 SVF for artificial fisheye pictures with cumulatively visible rings

Regarding the results coming from the evaluation of the artificial fisheye pictures (Fig. 8), the values differ again. The results of BMSkyView, a member of the above established group 2, follow the reference values of the calculated Steyn-method quite precisely, RayMan, member of group 1, again gives differing SVF values.

### 4.3. Upgrade

After the evaluation of the real and artificial fisheye pictures, the results pointed to a systematic deviation between the used software. As the members of group 2 were developed independently and correspond also very well to the mathematical reference, the members of group 1 were to be checked. It was found that Lambert's Law of radiation (also known as the cosine-law), was not included in RayMan and SkyHelios because of a

different interpretation of SVF. After providing a possibility to include Lambert's law via activating a checkbox, the same calculations were done once more with SkyHelios and the two groups are no longer to be distinguished (Fig. 9).
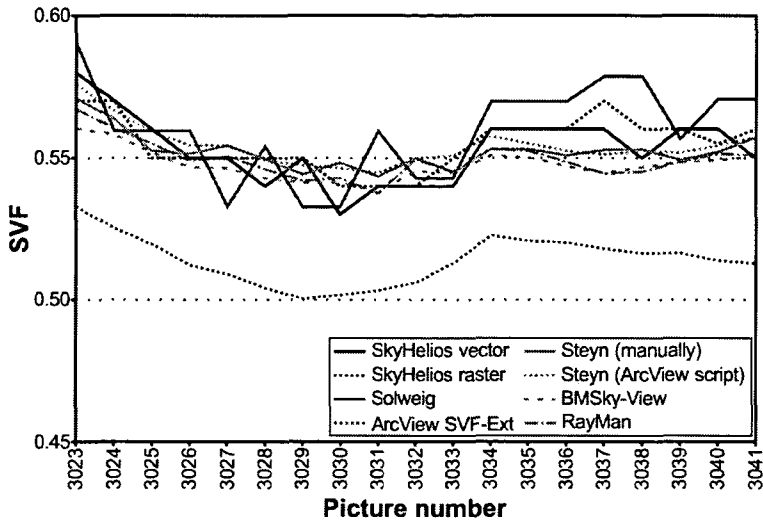


Fig. 9 SVF-diagram for transect 3 with extended SkyHelios and RayMan

## 5. CONCLUSION

In order to compare different methods and models which calculate the sky view factor, a set of already available programs were used as well as a manual method. To dispose of the manual method's disadvantages, a new Avenue Script was developed that can be used easily as a supplement for the ArcView GIS-software. The Script offers a fast and handy way of evaluating fisheye pictures directly on the computer screen and delivers reasonable results corresponding well to the other methods.

Also, a systematic gap in the obtained SVF values was found. After adjusting the respective software, all results show high accordance.

Considering the above results, a discussion has been started about the understanding and use of the sky view factor: Would it make sense to define the sky view factor in different ways, depending on the task and field of use?

In urban climatology for example, the cosine weighting is crucial because in urban environments it is mainly plain areas which are analyzed (streets, squares, etc.). Horizontally incoming radiation passes by without adding energy to the observed area, i. e. it plays an insignificant role.

Biometeorology on the other hand deals with bodies which receive for a big part radiation via horizontal radiation fluxes. A cosine weighting would neglect horizontal energy fluxes which in this case is inappropriate.

In any case it can be stated that controlling and cross-checking SVF-calculations is indispensable. This goes above all for checking theoretical models using virtual data by the help of real fisheye pictures. In models and in virtual data there can always be some errors, but fisheye pictures offer an inventory of the real situation.

## REFERENCES

Gál T, Rzepa M, Gromek B, Unger J (2007) Comparison between sky view factor values computed by two different methods in an urban environment. Acta Climatol Chorol Univ Szegediensis 40-41:17-26

Gál T, Lindberg F, Unger J (2009) Computing continuous sky view factors using 3D urban raster and vector databases: comparison and application to urban climate. Theor Appl Climatol 95:111-123

Grimmond CSB, Potter SK, Zutter HN, Souch C (2001) Rapid methods to estimate sky view factors applied to urban areas. Int J Climatol 21:903-913

Holmer B, Postgård U, Eriksson M (2001) Sky view factors in forest canopies calculated with IDRISI. Theor Appl Climatol 68:33-40

Lin TP, Matzarakis A, Hwang RL (2010) Shading effect on long-term outdoor thermal comfort. Build Environ 45:213-211

Lindberg F, Thorsson S, Holmer B (2008) SOLWEIG 1.0 – Modelling spatial variations of 3D radiant fluxes and mean radiant temperature in complex urban settings. Int J Biometeorol 52:697-713

Matuschek O, Matzarakis A (2010) Estimation of sky view factor in complex environment as a tool for applied climatological studies. In: Matzarakis A, Mayer H, Chmieliewski FM (eds) Proceed 7th Conf on Biometeorology. Berichte des Meteorologischen Instituts der Albert-Ludwigs-Universität Freiburg 20:534-539

Matzarakis A (2001) Die thermische Komponente des Stadtklimas. Berichte des Meteorologischen Institutes der Universität Freiburg. Nr. 6

Matzarakis A, Matuschek O (2010) Sky view factor as a parameter in applied climatology – rapid estimation by the SkyHelios model. Meteorol Zeitschrift 20:39-45

Matzarakis A, Rutz F, Mayer H (2007) Modeling radiation fluxes in simple and complex environments – application of the RayMan model. Int J Biometeorol 51:323-334

Matzarakis A, Rutz F, Mayer H (2010) Modeling radiation fluxes in simple and complex environments – basics of the RayMan model. Int J Biometeorol 54:131-139

Oke TR (1981) Canyon geometry and the nocturnal urban heat island: comparison of scale model and field observations. J Climatol 1:237-254

Oke TR (1987) Boundary layer climates. Methuen, London

Ratti C, Richens P (1999) Urban texture analysis with image processing techniques. In: Augenbroe G, Eastman Ch (eds) Proceed 8th Int Confon Computer Aided Architectural Design Futures held in Atlanta, Georgia

Richert C (2010) GIS-gestützte Analyse des klimatischen Potentials der Windenergie in der Region Freiburg im Breisgau auf der Grundlage von Messungen und Klimasimulationen. Magister Scientiarum Thesis, unpublished, Albert-Ludwigs-University of Freiburg, Freiburg

Rzepa M, Gromek B (2006) Variability of sky view factor in the main street canyon in the center of Łódź. Preprints Sixth Int Conf on Urban Climate, Göteborg, Sweden. 854-857

Stewart I (2009): Classifying urban climate field sites by "Local Climate Zones". IAUC Urban Climate News 34:8-11

Steyn DG (1980) The calculation of view factors from fisheye-lens photographs. Atmos-Ocean 18:245-258

Unger J (2004) Intra-urban relationship between surface geometry and urban heat island: review and new approach. Climate Res 27:253-264

Unger J (2006) Modelling the annual mean maximum urban heat island with the application of 2 and 3D surface parameters. Climate Res 30:215-226

Unger J (2009) Connection between urban heat island and sky view factor approximated by a software tool on a 3D urban database. Int J Environ Pollution 36:59-80

VDI (1998) VDI 3787, Part I: Environmental Meteorology, Methods for the human biometeorological evaluation of climate and air quality for the urban and regional planning at regional level. Part I: Climate. Beuth, Berlin